# Influence of archwire and bracket dimensions on sliding mechanics: derivations and determinations of the critical contact angles for binding

## Robert P. Kusy and John Q. Whitley

Dental Research Center, School of Dentistry, University of North Carolina, USA

SUMMARY   There is every indication that classical friction controls sliding mechanics below some critical contact angle, $\theta_c$. Once that angle is exceeded, however, binding and notching phenomena increasingly restrict sliding mechanics. Using geometric archwire and bracket parameters, the $\theta_c$ is calculated as the boundary between classical frictional behaviour and binding-related phenomena. What these equations predict is independent of practitioner or technique. From these derivations two dimensionless numbers are also identified as the bracket and the engagement index. The first shows how the width of a bracket compares to its Slot; the second indicates how completely the wire fills the Slot. When nominal wire and bracket dimensions are calculated for both standard Slots, the maximum $\theta_c$ theoretically equals 3.7 degrees. Thus, knowledge of the archwire or bracket alone is insufficient; knowledge of the archwire-bracket combination is necessary for $\theta_c$ to be calculated. Once calculated, sliding mechanics should be initiated only after the contact angle, $\theta$, approaches the characteristic value of $\theta_c$ for the particular archwire-bracket combination of choice—that is, when $\theta \approx \theta_c$.

## Introduction

Recently, Kusy and Whitley (1997) stated that the resistance to sliding (RS) may be partitioned into three components: classical friction (FR), binding (BI), and notching (NO):

$$RS = FR + BI + NO. \qquad (1)$$

Over 20 years ago, classical friction (FR) was further subdivided into ploughing (PL), roughness interlocking (IN), and shearing (SH) components (Jastrzebski, 1976):

$$FR = PL + IN + SH. \qquad (2)$$

When these concepts are combined, equations (1) and (2) constitute the general expression of resistance to sliding,

$$RS = PL + IN + SH + BI + NO, \qquad (3)$$

which is applicable to both the passive and active configurations.

In the passive configuration (Kusy and Whitley, 1997), where the contact angle ($\theta$) (Proffit, 1993) between archwire and bracket Slot is less than some critical contact angle ($\theta_c$), only classical friction is important because binding (Frank and Nikolai, 1980; Kapila *et al.*, 1990) and notching (Hansen *et al.*, 1998) are non-existent. That is,

$$RS = PL + IN + SH = FR. \qquad (4)$$

Over the last 10 years the orthodontic literature has documented classical friction in various archwire-bracket combinations as a function of archwire-bracket materials (Angolkar *et al.*, 1990; Kapila *et al.*, 1990; Kusy and Whitley, 1990a; Pratten *et al.*, 1990; Tselepis *et al.*, 1994), physical dimensions (Frank and Nikolai, 1980; Tidy, 1989; Kusy *et al.*, 1991), surface roughness (Kusy and Whitley, 1990a,b; Prososki *et al.*, 1991), fluid medium (Tidy, 1989; Saunders and Kusy, 1994; Kusy and Schafer, 1995), and surface

modification (Kusy *et al.*, 1992, 1997; Saunders and Kusy, 1993). In addition, Nanda and Ghosh (1997) have recently presented a thorough review of the subject.

Although passive configuration has been extensively researched, the active configuration (Kusy and Whitley, 1997) has received considerably less attention, primarily because of the experimental difficulties associated with measuring θ at angles greater than 0 degrees. What is at least implicitly known (Peterson *et al.*, 1982) is that binding increasingly plays a role as θ increases. In this regard it is believed that three stages exist:

1. In the early stage, when θ either just equals or just exceeds $\theta_c$ (i.e. $\theta \geq \theta_c$), classical friction and binding solely contribute to the resistance to sliding so that equation (3) reduces to,

$$RS = PL + IN + SH + BI = FR + BI. \quad (5)$$

Under these circumstances sliding is somewhat impeded, although neither classical friction nor binding dominates the other and notching is negligible.

2. In the intermediate stage, when θ is clearly greater than $\theta_c$ (i.e. $\theta > \theta_c$), binding increasingly restricts sliding as classical friction becomes only a small part of binding (i.e. BI >> FR). Thus, equation (5) reduces to,

$$RS \approx BI \quad (6)$$

3. In the late stage, when θ is much greater than $\theta_c$ ($\theta >> \theta_c$), both classical friction and binding become negligible relative to notching (i.e. NO >> BI >> FR). As a consequence, sliding is impossible, as this special case of binding makes RS approach infinity. Thus, equation (3) simplifies to,

$$RS \approx NO \approx \infty. \quad (7)$$

From the preceding three stages that exist in the active configuration, three topical areas may be identified: the binding phenomenon, the notching phenomenon, and the critical contact angle. Although binding has been formalized in terms of a superposition principle (Articolo and Kusy, 1997) and notching is under investigation both from the viewpoint of cataloguing its morphological features and identifying its causal

relationships (Kusy and Whitley, 1997), little is known about the nature of $\theta_c$, and specifically when it occurs and how it is influenced. In this investigation two theoretical equations are first derived so that the practical means and bounds of $\theta_c$ may be determined in terms of the nominal archwire-bracket parameters. These results show that sliding mechanics will become increasingly difficult, when $\theta_c$ exceeds a specific value that can be determined by geometric parameters. That maximum value never exceeds $\theta_c \approx 4$ degrees, regardless of the archwire-bracket couple, wire technique, or practitioner involved, or else binding will increasingly restrict sliding [cf. equations (5) and (6)] until sliding stops altogether [cf. equation (7)]. In the final analysis, this maximum value may be modified into a simple, practical equation.

**Theoretical determinations**

The underlining premise is that sliding principally occurs in the passive configuration (Figure 1, top), that is, when the effective archwire size ('Size') is less than the bracket Slot ('Slot'). This premise may be mathematically defined by the clearance ('Delta') as,

$$Delta = Slot - Size > 0.$$

At the instant when the angulation (or for that matter, the torque) makes the archwire effectively fill the Slot,

$$Delta = Slot - Size = 0,$$

binding is imminent as the critical contact angle ($\theta_c$) has been achieved. This active configuration (Figure 1, bottom) is a function of only one other parameter, the bracket width ('Width'). By manipulating Slot, Size, and Width, the $\theta_c$ beyond which binding will increasingly obstruct sliding mechanics can be written as (cf. Appendix I):

$$\theta_c = \cos^{-1} \frac{(Size)^2 - (Width)^2}{(Size)(Slot) \pm ((Width)^2 (-(Size)^2 + (Slot)^2 + (Width)^2))^{0.5}}. \quad (AI9)$$

Although readily manageable with today's high speed computers, nonetheless, the physical
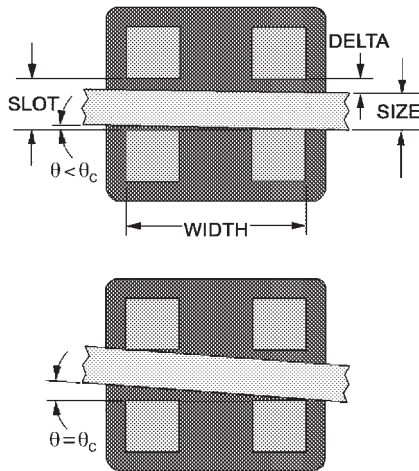
**Figure 1** Schematic illustrations of an archwire-bracket couple: in the passive configuration, when $\theta < \theta_c$ (top)—that is, when the contact angle ($\theta$) is less than the critical contact angle ($\theta_c$) as a result of angulation; and in the active configuration, when $\theta \geq \theta_c$ (bottom). Together these illustrations define the three geometric parameters of importance (Size, Slot, and Width), the wire-bracket clearance (Delta = Slot – Size), and the relationship of $\theta$ to $\theta_c$.

interpretation of this equation is difficult to comprehend. For example, how should the computations be plotted, and what practical dimensionless indices should be considered? These answers can be obtained if an equivalent theoretical expression for $\theta_c$ is derived as (cf. Appendix II):

$$\frac{Size}{Slot} = -\frac{Width}{Slot}(\sin \theta_c) + \cos \theta_c. \quad (AII3)$$

In equation (AII3) the Size/Slot defines the engagement index as the ratio of the archwire size to the bracket Slot. This index defines the fraction of the bracket Slot that is filled by the archwire (Figure 1, top). Equation (AII3) also defines a second index, the bracket index. This equals the ratio of Width/Slot, or equivalently, the number of times that the bracket is wider than its Slot dimension (Figure 1, top). Together, these dimensionless indices define all that is necessary to determine $\theta_c$ as the point at which binding initiates.
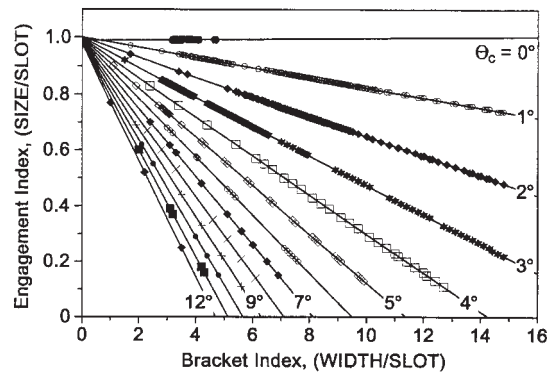


**Figure 2** Determination of theoretical values of bracket index-engagement index plots at discrete values of $\theta_c$ (cf. equations AI9 and AII3, and Appendices I and II, respectively). These lines represent the linear regressions of compiled data that were obtained from $\theta_c = 0$ degrees to $\theta_c = 12$ degrees at 1 degree increments. Note that although the slopes of successive lines vary by a constant increment of –0.0175, the intercepts depart more from 1.0 as $\theta_c$ increases from 0 degrees to 12 degrees.

Equation (AII3) also indicates how the data should be plotted. Recalling the formula for a straight line, $Y = mX + b$, the following characteristics should be plotted:

1. On the *X*-axis plot, the bracket index as the Width/Slot.
2. On the *Y*-axis plot, the engagement index as the Size/Slot.

When these indices are plotted, the slope and intercept of each line will equal $-\sin \theta_c$ and $\cos \theta_c$, respectively [cf. equation (AII3)]. When plotted, the exact solution of equation (AI9) via computer appears as shown in Figure 2.

**Practical determinations**

Although mathematically exact, the boundaries of 0–16 for the bracket indices and 0–1.0 for the engagement indices exceed today's practical limits. Reference to nominal parameters in units of one thousandth of an inch called mils (Table 1) indicate that the Widths can vary from 250 mils for 1's, the central incisors to close diastemas, to 125 mils for canines and premolars to close extraction sites. The Sizes can vary from 14, 16,

**Table 1** Nominal parameters of archwires and brackets that are used in sliding mechanics.

|  | For an 18 Slot × 1000 (″)* (0.46)** | For a 22 Slot × 1000 (″) (0.56) |
|---|---|---|
| Width | 125 or 250 (3.18 or 6.35) | 125 or 250 (3.18 or 6.35) |
| Size | 14[†] (0.36) | 14 (0.36) |
|  | 16[‡] (0.41) | 16[‡] (0.41) |
|  | 16 × 16[‡] (0.41 × 0.41) | 18[‡] (0.46) |
|  | 16 × 22[‡] (0.41 × 0.56) | 16 × 16[‡] (0.41 × 0.41) |
|  |  | 16 × 22[‡] (0.41 × 0.56) |
|  |  | 17 × 25 (0.43 × 0.64) |
|  |  | 18 × 25 (0.46 × 0.64) |
|  |  | 19 × 25 (0.48 × 0.64) |

*Expressed in mils.
**Equivalent value expressed in mm.
[†]Questionable to slide on.
[‡]Most popular to slide on.

16 × 16, and 16 × 22 mils for both Slots and also include the 17 × 25, 18, 18 × 25, and 19 × 25 mils for the 22 mils Slot. Note that, from this point forward, the unit of mils will be implicitly understood in the text, although the equivalent mm values may also be referenced from Table 1.

To determine the practical boundaries of the theoretical plot (cf. Figure 2), the maxima and minima of the bracket indices must be calculated as follows (Table 1):

1. For the maximum bracket index, the largest bracket Width and the smallest bracket Slot must be chosen. In principle, that is a 250/18 = 13.9.
2. For the minimum bracket index, the smallest Width and the largest Slot must be chosen. That is a 125/22 = 5.7.

On this basis the bracket indices may range from 5 to 14.

Using the same approach, the maxima and minima of the engagement indices must be calculated as follows (Table 1):

1. For the maximum engagement index, the largest archwire Size and the smallest bracket Slot must be one of two practical combinations—either a 16/18 = 0.89 or a 19/22 = 0.86.
2. For the minimum engagement index the smallest Size and the largest Slot must equal a 14/22 = 0.64.

On this basis the engagement indices need only range from 0.6 to 0.9, although 0.5 to 1.0 will be shown. Note that the range is extended in case a practitioner wishes to use a wire that fills the Slot (e.g. an 18 × 25 Size in an 18 Slot for a Size/ Slot = 18/18 = 1.0) or to use an archwire that is smaller than a 14 (e.g. a 12 Size in a 22 Slot for a Size/Slot = 12/22 = 0.55).

When the nominal parameters of archwires and brackets, which are used in sliding mechanics, are now superimposed onto the upper right-hand quadrant of the theoretical plot (cf. Figure 2), Figure 3 results. Note that only four discrete bracket indices are indicated having Width/Slot ratios of 125/22, 125/18, 250/22, and 250/18. Also note that seven engagement indices exist: two Size/Slot ratios for the 18 Slot (14/18 and 16/18) and five Size/Slot ratios for the 22 Slot (14/22, 16/22, 17/22, 18/22, and 19/22). Associating only either the 18 Slot or 22 Slot data, the 14 points represent the current practical sliding combinations, and the connecting lines show how $\theta_c$ will change as the bracket Width increases from 125 to 250. Recalling that a higher value of $\theta_c$ means that sliding will occur despite more misalignment, three important observations may be gleaned from the practical plot of Figure 3, while maintaining everything else equal:

1. Narrower bracket Widths at least double the values of $\theta_c$s. This benefit is countered by the long-standing observation that narrower brackets are harder to control than wider ones.
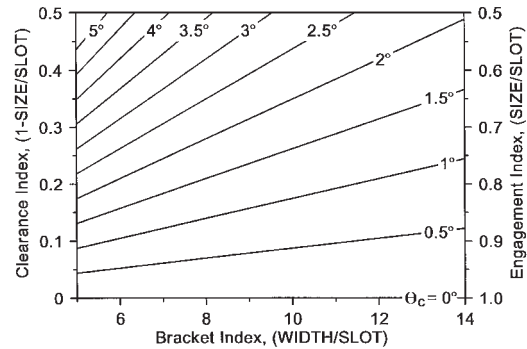2. Smaller bracket Slots require that the clinician be as much as 25 per cent more
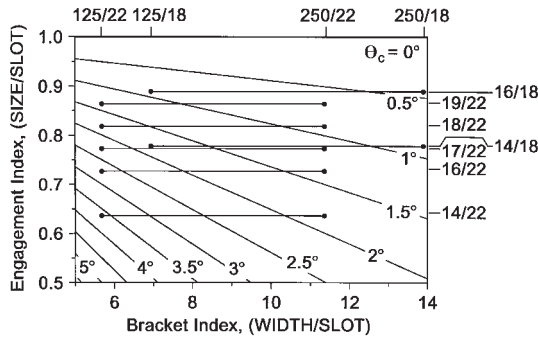
**Figure 3** Computations of nominal values of bracket index-engagement index plots (●—●) superimposed on the discrete values of $\theta_c$ (cf. equations (AI9) & (AII3) and Appendices I & II, respectively). Each datum (●) corresponds to a particular bracket Width to bracket Slot ratio (i.e. the bracket index); whereas, the interconnecting horizontal lines (—) represent a particular archwire Size to bracket Slot ratio (i.e. the engagement index). Based on these nominal values, the maximum $\theta_c$ is always ≤3.7 degrees.



**Figure 4** Determination of practical values of bracket-engagement index plots (and its associated bracket-clearance index plots) at discrete values of $\theta_c$ (cf. equation AIII5 and Appendix III). Use this plot to determine $\theta_c$ for each archwire-bracket combination.

precise in initial alignment and levelling or else binding will occur. This outcome suggests that inexperienced clinicians will find the 22 Slot more suitable for sliding mechanics.

3. Smaller wire Sizes can substantially facilitate the initiation of sliding mechanics. For example, for a 16 Size wire in a bracket having a 22 Slot and an 125 Width, the $\theta_c = 2.8$ degrees. This 16/22 engagement index should be contrasted with the 16/18 engagement index wherein $\theta_c = 0.9$ degrees. Although both the bracket Width and wire Size are identical, the 22 Slot allows $\theta_c$ to be three times as large as that of the 18 Slot.

To summarize Figure 3, even in the best case scenario the practitioner must align and level so that the angulation between wire and bracket is within 3.7 degrees or else binding will increasingly occur until sliding ceases altogether. To accomplish that best case scenario most easily within the strength and stiffness requirements of the appliance, the bracket Width and wire Size should be small, and the bracket Slot should be large. Although the use of a smaller Slot is possible, the precision must be greater prior to initializing sliding mechanics.

In the final analysis the theoretical requirement to align and level to within about 4 degrees prior to sliding enables equation (AII3) to be simplified without any clinically significant loss of accuracy. Using the approximations that $\sin \theta_c \approx \pi\, \theta_c/180$ and $\cos \theta_c \approx 1$, substitution of these quantities into equation (AII3) and rearrangement yields the simple, practical equation (cf. Appendix III),

$$\theta_c = \frac{57.32\,[1 - (\text{Size/Slot})]}{(\text{Width/Slot})}. \qquad \text{(AIII5)}$$

Now $\theta_c$ can be expressed as the product of a constant times one minus the engagement index (i.e. the clearance index—the fraction of the bracket Slot that is not filled by the archwire) divided by the bracket index. For convenience, equation (AIII5) is plotted in Figure 4 using either the engagement or clearance indices against the bracket index.

**Future work**

Future investigations of $\theta_c$ will compare bracket and engagement indices of select manufactured archwire-bracket combinations to these theoretical nominal values. In addition, $\theta_c$s will be assessed for select manufactured archwire-bracket combinations in terms of their actual

calculated values and experimental measurements, the latter being determined by their specific resistances to sliding at several $\theta$s. Thereby, the role of classical friction and binding will be more fully elucidated.

## Conclusions

Using only wire Size, bracket Slot, and bracket Width dimensions, theoretical equations (AI9) and (AII3) can be derived that describe the value at which any critical contact angle ($\theta_c$) is attained. Thus, this angle at which binding increasingly prevents sliding mechanics from occurring may be determined.

The derivation of the $\theta_c$ equations shows that there are two indices of importance: the engagement index, which expresses the ratio of the wire Size to the bracket Slot; and the bracket index, which expresses the ratio of the bracket Width to its Slot. Knowledge of both the archwire and the bracket is required for sliding mechanics to be understood.

For nominal wire and bracket dimensions the boundaries of the bracket index versus engagement index suggest that $\theta_c$ must lie between 0 and approximately 4 degrees for sliding to occur. Given this limited range of $\theta_c$, a simple practical equation (AIII5) can be derived. Within this range the wider brackets restrict sliding mechanics by reducing $\theta_c$.

## Address for correspondence

Professor Robert P. Kusy
University of North Carolina
DRC Building 210H
CB# 7455
Chapel Hill
NC 27599, USA

## Acknowledgements

## References

Angolkar P V, Kapila S, Duncanson M G Jr, Nanda R S 1990 Evaluation of friction between ceramic brackets and orthodontic wires of four alloys. American Journal of Orthodontics and Dentofacial Orthopedics 98: 499–506

Articolo L C, Kusy R P 1997 Influence of angulation on binding of orthodontic materials during sliding. Journal of Dental Research 76: 197 (Abstract)

Frank C A, Nikolai R J 1980 A comparative study of frictional resistances between orthodontic bracket and archwire. American Journal of Orthodontics 78: 593–609

Hansen J D, Kusy R P, Saunders C R 1998 Archwire damage from ceramic brackets via notching. Orthodontic Review (in press)

Jastrzebski Z D 1976 The nature and properties of engineering materials, 2nd edn. Wiley & Sons, New York, pp. 182–185

Kapila S, Angolkar P V, Duncanson M G Jr, Nanda R S 1990 Evaluation of friction between edgewise stainless steel brackets and orthodontic wires of four alloys. American Journal of Orthodontics and Dentofacial Orthopedics 98: 117–126

Kusy R P, Schafer D L 1995 Effect of salivary viscosity on frictional coefficients of orthodontic archwire/bracket couples. Journal of Materials Science: Materials in Medicine 6: 390–395

Kusy R P, Whitley J Q 1990a Coefficients of friction for archwires in stainless steel and polycrystalline alumina bracket slots. I: the dry state. American Journal of Orthodontics and Dentofacial Orthopedics 98: 300–312

Kusy R P, Whitley J Q 1990b Effects of surface roughness on the coefficients of friction in model orthodontic systems. Journal of Biomechanics 23: 913–925

Kusy R P, Whitley J Q 1997 Friction between different wire-bracket configurations and materials. Seminars in Orthodontics 3: 166–177

Kusy R P, Whitley J Q, Prewitt M J 1991 Comparison of the frictional coefficients for selected archwire bracket slot combinations in the dry and wet states. Angle Orthodontist 61: 293–302

Kusy R P, Tobin E J, Whitley J Q, Sioshansi, P 1992 Frictional coefficients of ion-implanted alumina against ion-implanted beta titanium in the low load, low velocity, single pass regime. Dental Materials 8: 167–172

Kusy R P, Saunders C R, Whitley J Q 1997 Improving arch mechanics through surface chemistry. In: Nanda R (ed.) Biomechanics in clinical orthodontics. W B Saunders Company, Philadelphia, pp. 50–64

Nanda R, Ghosh J 1997 Biomechanical considerations in sliding mechanics. In: Nanda R (ed.) Biomechanics in clinical orthodontics. W B Saunders Company, Philadelphia, pp. 188–217

Peterson L, Spencer R, Andreasen G F 1982 A comparison of frictional resistance of Nitinol and stainless steel wires in Edgewise brackets. Quintessence International Digest 13: 563–571

Pratten D H, Popli K, Germane N, Gunsolley J 1990 Frictional resistance of ceramic and stainless steel orthodontic brackets. American Journal of Orthodontics and Dentofacial Orthopedics 98: 398–403

Proffit W R 1993 Contemporary orthodontics, 2nd edn. Mosby Year Book, St. Louis, p. 306

Prososki R P, Bagby M D, Erickson L C 1991 Static frictional force and surface roughness of nickel-titanium archwires. American Journal of Orthodontics and Dentofacial Orthopedics 100: 341–348

Saunders C R, Kusy R P 1993 Surface modification methodologies for polycrystalline alumina: effects on morphology and frictional coefficients. Journal of Materials Science: Materials in Medicine 4: 422–430

Saunders C R, Kusy R P 1994 Surface topography and frictional characteristics of ceramic brackets. American Journal of Orthodontics and Dentofacial Orthopedics 106: 76–87

Tidy D C 1989 Frictional forces in fixed appliances. American Journal of Orthodontics and Dentofacial Orthopedics 96: 249–254

Tselepis M, Brockhurst P, West V C 1994 Frictional resistance between brackets and archwires. American Journal of Orthodontics and Dentofacial Orthopedics 106: 131–138

## Appendix I
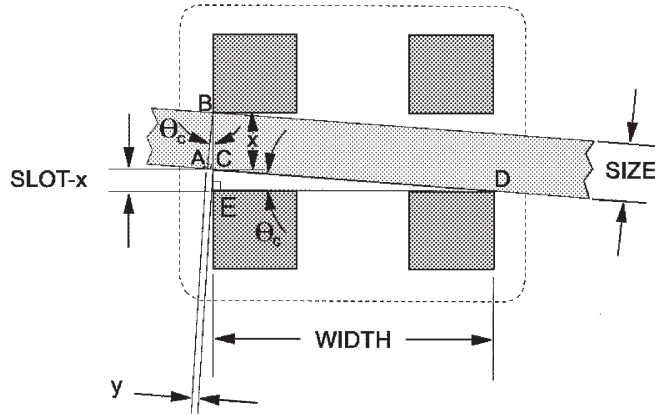


**Figure 5** Schematic drawing of the relationship between an archwire and a bracket in terms of the wire Size, bracket Slot and Width, and $\theta_c$. For clarity only the four tie-wings of the bracket are highlighted; the retention pad is shown as a dashed line. Note also that two dummy parameters ($x$ and $y$) and two similar triangles (ABC and EDC) are introduced.

To derive this critical condition, reference must be made to Figure 5, in which two similar triangles, ABC and EDC, must be identified in which '$x$' and '$y$' represent two dummy variables. Because these are similar triangles,

$$\overline{AB}/\overline{AC} = \overline{ED}/\overline{EC}$$

or

$$\text{Size}/y = \text{Width}/(\text{Slot} - x) \tag{AI1}$$

From the Pythagorean Theorem,

$$(\overline{BC})^2 = (\overline{AB})^2 + (\overline{AC})^2,$$

or

$$(x^2) = (\text{Size})^2 + (y)^2,$$

so that

$$y = [x^2 - (\text{Size})^2]^{0.5} \tag{AI2}$$

Substituting equation (AI2) into equation (AI1),

$$\text{Size}/[x^2 - (\text{Size})^2]^{0.5} = \text{Width}/(\text{Slot} - x)$$

Squaring both sides of the expression,

$$(\text{Size})^2/[x^2 - (\text{Size})^2] = (\text{Width})^2/(\text{Slot} - x)^2$$

After expanding,

$$(\text{Size})^2/[x^2 - (\text{Size})^2] = (\text{Width})^2/[(\text{Slot})^2 - 2\,(\text{Slot})x + x^2]$$

and applying the distributive law,

$$(\text{Size})^2\,(\text{Slot})^2 - 2\,(\text{Size})^2\,(\text{Slot})\,x + (\text{Size})^2\,x^2 = (\text{Width})^2\,x^2 - (\text{Width})^2\,(\text{Size})^2$$

After rearranging,

$$(\text{Size})^2\,x^2 - (\text{Width})^2\,x^2 - 2\,(\text{Size})^2\,(\text{Slot})x + (\text{Size})^2\,(\text{Slot})^2 + (\text{Width})^2\,(\text{Size})^2 = 0,$$

or

$$[(\text{Size})^2 - (\text{Width})^2]x^2 + [-2\,(\text{Size})^2\,(\text{Slot})]x + [(\text{Size})^2\,(\text{Slot})^2 + (\text{Width})^2\,(\text{Size})^2] = 0$$

To simplify the mathematics, three dummy variables, $v$, $w$, and $d$ are now introduced and assigned as follows: $v = \text{Size}$, $w = \text{Slot}$, and $d = \text{Width}$,

$$(v^2 - d^2)x^2 + (-2v^2w)x + (v^2w^2 + d^2v^2) = 0 \tag{AI3}$$

Solving equation AI3 using the quadratic formula, $ax^2 + bx + c = 0$, in which

$$x = [-b \pm (b^2 - 4ac)^{0.5}]/2a$$

and $a$, $b$, and $c$ are the coefficients of the first, second, and third terms and equal $(v^2 - d^2)$, $(-2v^2w)$, and $(v^2w^2 + d^2v^2)$, respectively,

$$x = \frac{-(-2v^2w) \pm [(-2v^2w)^2 - 4(v^2 - d^2)\,(v^2w^2 + d^2v^2)]^{0.5}}{2(v^2 - d^2)}. \tag{AI4}$$

From triangle ABC (Figure 5),

$$\text{Size} = x\cos\theta_c,$$

so that

$$x = \text{Size}/\cos\theta_c = v/\cos\theta_c. \tag{AI5}$$

Substituting equation (AI5) into equation (AI4) and rearranging yields,

$$\theta_c = \cos^{-1}\frac{2v(v^2 - d^2)}{+2v^2w \pm [(-2v^2w)^2 - 4(v^2 - d^2)v^2\,(w^2 + d^2)]^{0.5}}. \tag{AI6}$$

Factoring out $2v$ yields,

$$\theta_c = \cos^{-1}\frac{(v^2 - d^2)}{vw \pm [(v^2w^2) - (v^2 - d^2)\,(w^2 + d^2)]^{0.5}}. \tag{AI7}$$

Simplifying the denominator gives,

$$\theta_c = \cos^{-1}\frac{(v^2 - d^2)}{vw \pm [d^2(-v^2 + w^2 + d^2)]^{0.5}}. \tag{AI8}$$

Finally, substituting the original definitions for $v$, $w$, and $d$ into equation (AI8) gives,

$$\theta_c = \cos^{-1} \frac{(Size)^2 - (Width)^2}{(Size)\,(Slot) \pm \{(Width)^2\,[-(Size)^2 + (Slot)^2 + (Width)^2]\}^{0.5}}. \tag{AI9}$$

Equation (AI9) defines the exact, closed form solution of the critical contact angle at which binding theoretically occurs as a function of archwire size, bracket slot, and bracket width.

## Appendix II

To derive the equivalent, theoretical equation the definition of the tangent function is applied to Figure 5 as:

$$\tan \theta_c = \sin \theta_c / \cos \theta_c = (\text{side opposite } \theta_c)/(\text{side adjacent } \theta_c).$$

The $\theta_c$ may be defined by the angle EDC in triangle EDC as

$$\tan \theta_c = \overline{EC}/\overline{ED} = (Slot - x)/Width. \tag{AII1}$$

Substituting equation (AI5) into equation (AII1) yields

$$\tan \theta_c = [Slot - (Size/\cos \theta_c)]/Width$$

By multiplying all terms by $\cos \theta_c$,

$$\sin \theta_c = [Slot\,(\cos \theta_c) - Size]/Width$$

and rearranging,

$$Size = -Width\,(\sin \theta_c) + Slot\,(\cos \theta_c). \tag{AII2}$$

Although equation AII2 requires an iterative solution, division by the Slot gives the dimensionless terms that are desired to understand the practical implications of the more cumbersome (and, hence, less comprehensible) equation AI9. Thus,

$$\frac{Size}{Slot} = -\frac{Width}{Slot}\,(\sin \theta_c) + \cos \theta_c. \tag{AII3}$$

## Appendix III

For $\theta_c \leq 5$ degrees equation (AII3) may be simplified by substituting $\sin \theta_c \approx \pi \theta_c/180$ and $\cos \theta_c \approx 1$ as shown below:

$$\frac{Size}{Slot} = -\frac{Width}{Slot}\,(\pi \theta_c/180) + 1. \tag{AIII1}$$

Multiplying by Slot/Width,

$$\frac{Slot}{Width}\frac{Size}{Slot} = -\pi \theta_c/180 + \frac{Slot}{Width}. \tag{AIII2}$$

Subtracting Slot/Width from both sides,

$$\frac{\text{Slot}}{\text{Width}}\frac{\text{Size}}{\text{Slot}} - \frac{\text{Slot}}{\text{Width}} = -\pi\theta_c/180. \tag{AIII3}$$

Multiplying by $-180/\pi$,

$$\theta_c = 180/\pi\left(-\frac{\text{Slot}}{\text{Width}}\frac{\text{Size}}{\text{Slot}} + \frac{\text{Slot}}{\text{Width}}\right). \tag{AIII4}$$

Factoring Slot/Width out of the right-hand terms of equation (AIII4) yields the simple, practical equation:

$$\theta_c = \frac{57.32[1 - (\text{Size/Slot})]}{(\text{Width/Slot})}. \tag{AIII5}$$